Bio-Medical Materials and Engineering 15 (2005) 367–374
IOS Press

Preliminary investigation of the feasibility of magnetic propulsion for future microdevices in blood vessels

Jean-Baptiste Mathieu [a,*], Sylvain Martel [a], L'Hocine Yahia [b], Gilles Soulez [c] and Gilles Beaudoin [c]

[a] *NanoRobotics Laboratory, École Polytechnique de Montréal, Montréal, PQ, H3C 3A7, Canada*
[b] *Group of Research in Biomechanics and Biomaterials, École Polytechnique de Montréal, Montreal, PQ, H3C 3A7, Canada*
[c] *Radiology Department, Faculty of Medicine, Université de Montréal, Montréal, PQ, H3C 3A7, Canada*

Received 10 May 2004

Abstract. The Magnetic Resonance Submarine (MR-Sub) project is a first attempt to validate a new propulsion method for future small magnetically controlled microdevices suited for minimally invasive applications in blood vessels. A Magnetic Resonance Imaging (MRI) system provides the driving force in three dimensions to a ferromagnetic core that could be embedded onto a specialised microdevice. The paper describes preliminary tests made to match the magnetic force induced by an MRI system on a ferromagnetic sphere with the drag force it encompasses in a cylindrical tube. These tests provide a proof of concept demonstrating that this new method of propulsion is very promising within the constraints of such types of operations. This conclusion is based on specific measurements showing that 1010/1020 carbon steel spheres (3.175 mm and 2.381 mm in diameter) can withstand a maximum flow of 0.370 ± 0.0064 l/min (19.5 cm/s) and 0.311 ± 0.01209 l/min (16.4 cm/s) respectively when placed inside a 6.35 mm diameter PMMA tube and subjected to a 18 mT/m magnetic field gradient.

Keywords: Magnetic resonance imaging, microdevice, magnetic propulsion

1. Introduction

A microdevice able to be controlled inside the blood vessels could potentially be used to perform several minimally invasive applications such as peripheral revascularization, highly localised drug delivery, tumour ablation or aneurysm embolisation, just to name a few. The level of miniaturisation of such a microdevice is a critical issue since smaller dimensions would allow more locations to be reached within the cardiovascular system. Micromotors or similar devices have been considered by other research groups as a mean of propulsion within the blood vessels. Unfortunately, the numerous moving parts and the lack of reliability of this approach, together with the limitations and size of a proper source of energy

*Corresponding author: Jean-Baptiste Mathieu, Nanorobotics Laboratory, lab# D-6160, Decelles building, École Polytechnique de Montréal, C.P. 6079 succ Centre-Ville, Montréal (Québec) Canada, H3C 3A7. Tel.: +1 514 340 4711, p. 5029; E-mail: jean-baptiste.mathieu@polymtl.ca.

make the design of a micromotor based propulsion system extremely complex. Present technologies impose serious constraints to realise a working device based on micromotors within an acceptable level of miniaturisation for operations within the blood vessels. For instance, the smallest ultrasonic motors presently available with an overall length of 1.5 mm and a diameter of 1.4 mm [10], are already too large for such applications [11]. After extensive reviews, we concluded that the simplest and most promising propulsion approach to achieve a sufficient level of miniaturisation while providing enough propulsion force was to rely on an external magnetic field acting on a small ferromagnetic core. Researches on magnetic propulsion for minimally invasive surgery have been conducted at the University of Virginia [3,7, 8] and at Tohoku University [12–14]. The concept studied at the University of Virginia aims at moving a ferromagnetic thermoseed (Video Tumor Fighter, VTF) through brain tissue in order to reach a brain tumour. Once the tumour is penetrated, the thermoseed is heated via eddy current using RF excitations and moved to scan and destroy the whole tumour volume. Propulsion is achieved by applying magnetic field gradients (hence a magnetic force) generated by the Magnetic Stereotaxis System (MSS) which is a custom piece of equipment involving six supraconducting coils and a fluoroscopic imaging system. The VTF requires 5 to 7 T/m magnetic field gradients to move the thermoseed straight through brain tissue. On the other hand, the device being propelled at Tohoku University consists of a screw shaped body (between 1 and 2 mm in diameter and 8 to 15 mm in length) with an embedded magnet. When applying a rotating magnetic field, the screw shaped device rotates and digs its path through tissues. The velocity of the screw shaped device is a function of the magnetic torque, rotational velocity of the field and the pitch of the screw.

Our microdevice will be propelled by an external magnetic force acting on it. This force is generated by magnetic field gradients as the device passes through the blood vessels. The physical parameters of the blood vessels determine the drag force and the constraints encompassed by the microdevice. The quantity and nature of ferromagnetic particles are determined according to the medical application to be performed. Knowing that the viscosity of the blood is lower than brain tissues, magnetic field gradients of less intensity than the ones considered at the University of Virginia can be used to induce a magnetic force strong enough to navigate against the blood flow. More interestingly, we found that the magnetic field and gradients used for imaging purposes in Magnetic Resonance Imaging (MRI) systems are strong enough for endovascular propulsion as envisioned in this paper. As such, the name MR-Sub has been selected to describe both the project and the microdevice.

The magnetic force applied on a ferromagnetic particle is proportional to its volume. The miniaturisation of the MR-Sub can be done by embedding a smaller quantity of ferromagnetic material which could take various forms including but not limited to ferromagnetic powder. As such, the size of the microdevice is greatly influenced by the rate of maximum blood flow expected. The blood flow varies with regard to the blood vessels used during travel. Another advantage of this method beside the fact that the process of miniaturisation of the microdevices is much simplified through the use of an external force generator (the MRI system), is that the steering of the microdevice can also be done simply by changing the direction of the magnetic field gradient vector $\nabla \vec{B}$. The smaller the embedded ferromagnetic structure is, the smaller the microdevice can be and the wider its operating range becomes. As a matter of fact, it could potentially, depending on the operations and the force required, gain access to the capillaries if necessary. Combined operations can also be envisioned. For instance, MR-Sub could also be released near the treatment area through a catheter. Then, it could be controlled using a control software able to track it, compute its trajectory and then determine the magnetic field gradient to be applied on it. It is clear that this magnetic propulsion concept is extremely promising for miniaturised systems targeted at *in vivo* applications. As such, this paper describes the results of our preliminary MRI

control tests that validate some of the fundamental theoretical calculations by experimentations where magnetic and drag forces were confronted.

2. Background

The torque and the force induced by an MRI system can be calculated [4] from

$$\vec{\tau} = \vec{m} \times \vec{B} = V_{\text{ferro}} \cdot \vec{M} \times \vec{B}, \tag{1}$$

$$\vec{F}_{\text{magnetic}} = \vec{m} \cdot \nabla \vec{B} = V_{\text{ferro}} \cdot \vec{M} \cdot \nabla \vec{B}. \tag{2}$$

In Eqs (1) and (2), τ is the magnetic torque (N·m), $\vec{F}_{\text{magnetic}}$ is the magnetic force (N), $\vec{m}$ is the magnetic moment of the ferromagnetic body (A·m^2), $\vec{M}$ is the magnetisation of the material (A/m), V_{ferro} is the volume of the ferromagnetic body (m^3), $\vec{B}$ is the magnetic induction (T) and $\nabla \vec{B}$ is the gradient (spatial variation) of the magnetic induction (T/m).

The drag force (D) acting on a sphere in an infinite extent of fluid is given by [16]:

$$D = \frac{1}{2} \rho \cdot V^2 \cdot A \cdot C_D. \tag{3}$$

D is a function of the density of the fluid (ρ), relative velocity of the sphere to the fluid (V), frontal area of the sphere (A), drag coefficient (C_D) of a sphere in an infinite extent of fluid. Moreover, the drag coefficient (C_D) is a function of the Reynolds number (Re). As described in [15], the drag force on a rigid sphere falling in a rigid cylindrical tube depends on one more parameter which is the ratio of the diameter of the sphere to the diameter of the tube (d/D). The drag coefficient of a sphere falling in a cylindrical tube (C_{Dm}), is given in [15]:

$$C_{\text{Dm}} = C_D \times f^2. \tag{4}$$

The wall factor (f) is a function of Re and d/D. It is defined as the ratio between the terminal velocity of a sphere in an unbounded medium to the terminal velocity of the same sphere measured in a cylindrical tube.

In the scope of developing a magnetic propulsion system, the magnetic force must be stronger than the drag force on the microdevice for motion to take place and to allow control in displacement.

3. Materials and methods

The goal of the experiment was to verify if an MRI system could generate enough magnetic force on a ferromagnetic sphere in a cylindrical tube to make it withstand a water flow. The ferromagnetic samples used for the experiment were two 1010/1020 Carbon Steel spheres, 3.175 mm ($1/8''$) and 2.381 mm ($3/32''$) in diameter. The saturation induction $\vec{B}_{\text{sat}}$ of this alloy is 1.67 T and it is reached in a magnetising induction of 0.717 T. These magnetic properties were measured with a 155 Princeton Applied Research Corporation (PAR) vibrating sample magnetometer and 610 Hall Effect Bell Gaussmeter. All MRI tests

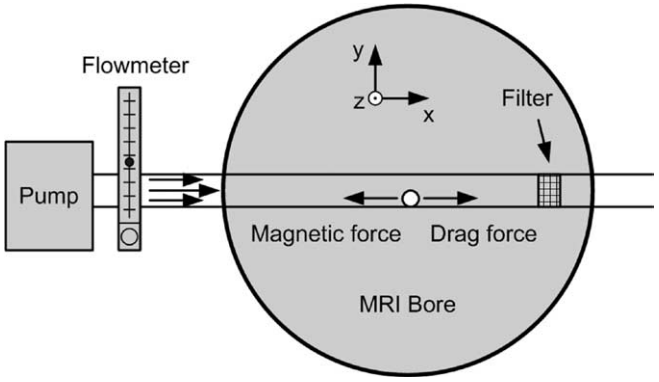

Fig. 1. Experimental set-up.

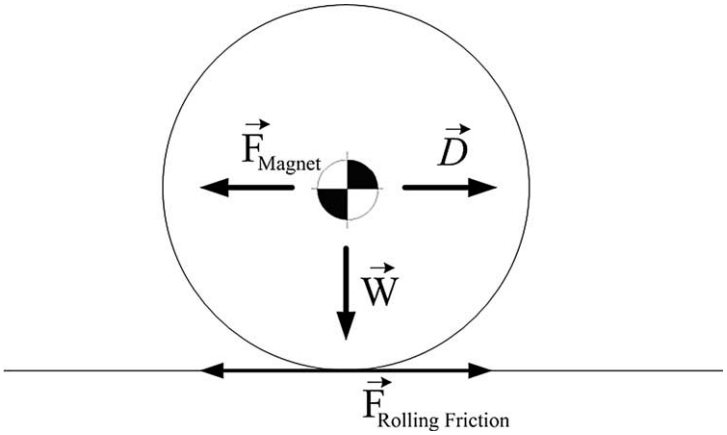

Fig. 2. Force diagram of the sphere lying on the PMMA tube.

were performed on a 1.5 T Siemens Magnetom Vision system. At this field intensity, the 1010/1020 carbon steel spheres are fully magnetised ($\vec{B}_{sat}$).

The water flow was pumped with a turbine pump placed outside of the MRI chamber. An 8 meters long flexible tubing was used to bring it to the centre of the MRI bore. There, the water flowed through a graduated, 6.35 mm inside diameter, 350 mm long PMMA cylindrical tube. The straight tube was placed along the x (transversal) direction of the MRI and the carbon steel sphere was placed inside of the tube. A filter was placed at the end of the tube in order to prevent the sphere to be carried away by the flow. The flow was measured and regulated with a variable-area flowmeter equipped with a flow control valve. The water flowing out of the MRI bore was brought back to the pump through flexible tubing. A schematic of the set-up is shown in Fig. 1. A pulsed magnetic field gradient of 18 mT/m was applied along the x direction of the MRI bore with a period of 12 ms with 10 ms on and 2 ms off. The magnetic field gradient was used in pulsed mode in order to allow the gradient coils to cool down since they cannot sustain continuous use under these conditions. The forces acting on the ferromagnetic sphere are the horizontal magnetic force, the drag force from the flow, the rolling friction, and weight. These forces are shown in Fig. 2. Figure 3 shows a photograph of the experimental set-up.

Flow measurements were taken as follows: the gradients were turned on while the valve of the flowmeter was opened completely in order to have maximum flow in the PMMA tube with the ferromagnetic

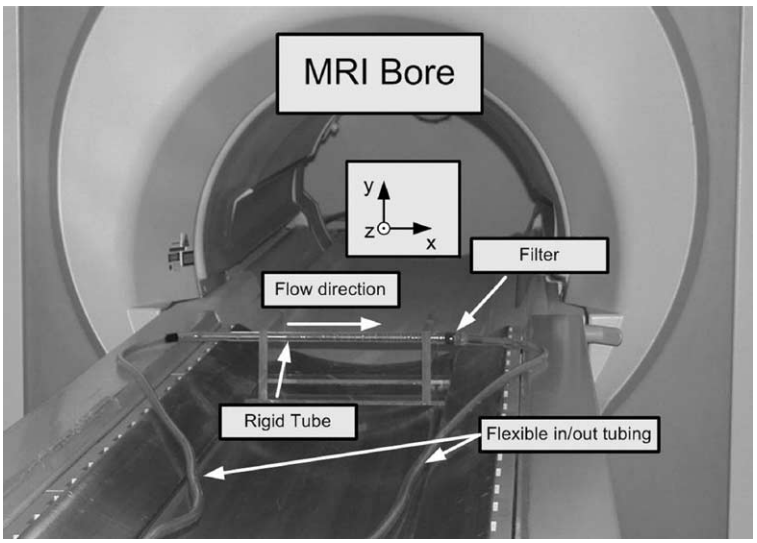

Fig. 3. Experimental set-up installed inside of 1.5 T Siemens Magnetom Vision MRI bore.

Table 1
Flow and mean velocity measurements

Sphere diameter (mm)	Flow (l/min) $\pm$ standard deviation	Mean velocity in tube (m/s) $\pm$ standard deviation
3.175	0.370 ± 0.006	0.195 ± 0.003
2.381	0.311 ± 0.012	0.164 ± 0.006

sphere resting on the filter. The valve of the flowmeter was then progressively closed until the sphere began moving against the flow. Finally the flow was adjusted until the sphere stopped moving and reached an equilibrium state. The motion of the sphere was monitored visually. The measurements were repeated 3 times with each sphere. The results of the equilibrium flow are recorded in Table 1. Mean velocity is calculated by dividing equilibrium flow by tube area.

4. Results and discussion

The experimental set-up was designed to simulate peripheral arteries at maximum systolic flow. Its diameter and flow are of the same order of magnitude as the ones that exist in the cardiovascular system. As shown by results in Table 1, a standard MRI system can generate enough magnetic force to move a ferromagnetic sphere inside a duct with properties close to real arteries (fluid density, flow, diameter, Reynolds number).

In an MRI system, a magnetised body tends to stay oriented in the direction of the field B_{o} (z direction). Therefore, it develops a resistance against any rotation that might reorient its magnetic domains. A rotation around the z-axis allows a magnetic body to spin without reorienting its magnetic domains. Hence, a magnetised sphere moving horizontally in the x direction rolls around the z-axis without magnetic resistance as shown in Fig. 4. On the contrary, when rolling implies a rotation around the x or y axis, a magnetized sphere slips instead of rolling. Rotations around the x or y-axis need to reorient the magnetic domains and such the magnetised body opposes a resistance to that motion. The straight tube

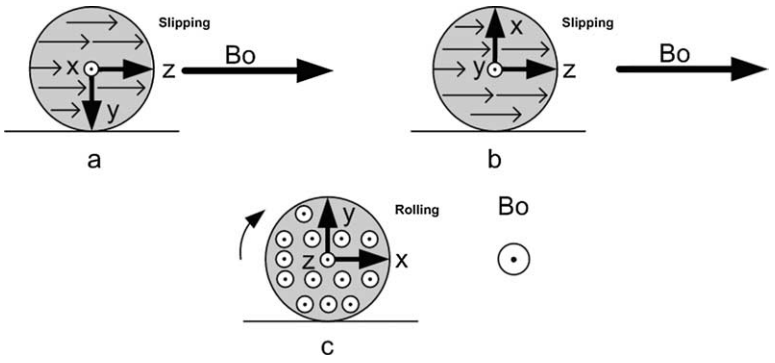

Fig. 4. A magnetized sphere will resist rolling around axis x (a) and y (b) because this motion implies its magnetic domains to be reoriented. Therefore, it tends to slip instead of rolling at the bottom of a tube. Rolling is not constrained when a sphere rotates around z (c) because this rotation can be made without reorienting the magnetic domains.

in the experiment was oriented along the x direction because it allows free rolling of the sphere. Friction is thus reduced since rolling friction coefficient is lower than slipping friction coefficient.

As the magnetic force is proportional to the gradient, existing MRI systems with 70 mT/m will provide 3.89 times more force. Using a ferromagnetic material with a stronger saturation magnetisation is another way to enhance the magnetic force. The samples used in these tests were 1010/1020 carbon steel with a saturation induction $\vec{B}_{\text{sat}}$ of 1.67 T. It is reported in the literature [1] that permendur (Fe49Co49Va2) provides the highest saturation induction ($\vec{B}_{\text{sat}} = 2.45$ T) [5]. A permendur sphere (diameter of 3.175 mm) submitted to a 70 mT/m gradient would encounter 5.71 times more magnetic force. Using an MRI system able to provide stronger magnetic field gradients and a better gradient coils cooling system could optimise the magnetic force. MRI systems with enhanced gradients systems will be needed in order to levitate the ferromagnetic sphere and solve the friction problems caused by rotations around the x and y axis.

According to [15], the drag coefficient of our spheres should be approximately 1.5 ($Re = 386$ and $d/D = 1/2$ for 3.175 mm sphere, $Re = 616$ and $d/D = 3/8$ for 2.381 mm sphere). However, our spheres are not falling in a quiescent fluid. They are subjected to a moving fluid and roll in the boundary layer at the bottom of the tube. The data provided in [15] cannot be used directly in our experimental set-up. However, it illustrates the parameters that influence the drag force acting on a sphere in a tube compared to a sphere in an infinite extent of fluid.

The tests described in this paper were made using water instead of blood as a fluid. The density of blood is 1.05 times higher than the density of water at the same temperature. As drag forces are proportional to the density of the fluid and as the blood has a Newtonian behaviour in vessels having a diameter higher than 1 mm [9], the drag forces should be 1.05 times stronger in blood.

The shape of the immersed body is also of primary concern. If it had been streamlined (ellipsoidal or drop shaped) and kept at the same volume (same magnetic force), its drag would have been lower and it would have been able to withstand a higher flow since its drag coefficient would have been lowered [16].

5. Conclusion

The experiments described in this paper show that magnetic propulsion relying on commercial MRI systems is possible. In the long term, hybrid MRI/magnetic propulsion systems providing more power-

ful gradient systems will allow the MR-Sub to be controlled in blood vessels conveying higher flows. Moreover, gradient coils cooling systems designed for continuous use would allow a constant magnetic force since the gradients would not need to be switched on and off periodically. The first advantage of a constant magnetic force is to make the magnetic control of the MR-Sub simpler. Another advantage of a constant gradient is a reduction of the rate of change of the magnetic field. As a matter of fact, fast variations in the magnetic field value could induce nerve stimulation and standards exist in each country to set a limit for the maximum $\mathrm{d}B/\mathrm{d}t$ [2].

The next steps in the project involve the development of a 3D real time position/control loop and to validate its use through experimentations with variable flow rates. Further studies will consider tubes with biological geometries and wall properties instead of straight and rigid walls. Combination of real time imaging with the driving gradients will be necessary. It was also observed that real-time and accurate positioning of the microdevice for control is currently limited due to ferromagnetic artefacts induced by the ferromagnetic material [6]. Although our group has made significant progress to compensate for such artefact errors, more efforts need to be done since positional errors could become a serious limitation to the feasibility of such a concept.

Acknowledgements

This work is supported in part by the Canada Research Chair (CRC) in Conception, Fabrication, and Validation of Micro/Nanosystems, by the Natural Sciences and Engineering Research Council of Canada (NSERC) and by Fond de la Recherche en Santé du Québec (FRSQ). We acknowledge the support of Hôpital Notre-Dame and Centre Hospitalier de l'Université de Montréal (CHUM) that provided infrastructure to conduct MRI tests. We also wish to thank Pr. Robert W. Cochrane from Physics department at the University of Montreal for allowing VSM magnetisation measurements.

References

[1] C.-W. Chen, *Magnetism and Metallurgy of Soft Magnetic Materials*, North-Holland, 1977.
[2] Environmental Health Directorate Health Protection Branch, Safety Code 26, Guidelines on Exposure to Electromagnetic Fields from Magnetic Resonance Clinical Systems, Canada, Minister of National Health and Welfare, 1987, 20 p.
[3] M.S. Grady, M.A. Howard 3rd, W.C. Broaddus, J.A. Molloy, R.C. Ritter, E.G. Quate and G.T. Gillies, Magnetic stereotaxis: a technique to deliver stereotactic hyperthermia, *Neurosurgery* **27** (1990), 1010–1015; discussion 1015–1016.
[4] J.D. Jackson, *Classical Electrodynamics*, 2nd edn, John Wiley and Sons, 1975.
[5] G. Lacroux, Les Aimants Permanents, Technique et Documentation, 1989.
[6] J.-B. Mathieu, S. Martel, L. Yahia, G. Soulez and G. Beaudoin, Preliminary studies for using magnetic resonance imaging systems as a mean of propulsion for microrobots in blood vessels and evaluation of ferromagnetic artefacts, Canadian congress on electric and computer engineering, 2003, Montreal, Canada, pp. 835–838.
[7] R.G. McNeil, R.C. Ritter, B. Wang, M.A. Lawson, G.T. Gillies, K.G. Wika, E.G. Quate, M.A. Howard 3rd and M.S. Grady, Functional design features and initial performance characteristics of a magnetic-implant guidance system for stereotactic neurosurgery, *IEEE Trans. Biomed. Eng.* **42** (1995), 793–801.
[8] R.G. McNeil, R.C. Ritter, B. Wang, M.A. Lawson, G.T. Gillies, K.G. Wika, E.G. Quate, M.A. Howard 3rd and M.S. Grady, Characteristics of an improved magnetic-implant guidance system, *IEEE Transactions on Biomedical Engineering* **42**(8) (1995), 802–807.
[9] W.R. Milnor, *Hemodynamics*, Williams and Wilkins, 1982.
[10] T. Morita, M.K. Kurosawa and T. Higuchi, Cylindrical micro-ultrasonic motor (stator transducer size: 1.4 mm in diameter and 5.0 mm long), *Ultrasonics* **38** (2000), 33–36.
[11] T. Morita, M.K. Kurosawa and T. Higuchi, Cylindrical shaped micro ultrasonic motor utilizing PZT thin film (1.4 mm in diameter and 5.0 mm long stator transducer) Sensors and Actuators, A: Physical: The 10th International Conference on Solid-State Sensors and Actuators TRANSDUCERS '99, 7–10 June 1999, **83** (1 May), (2000), 225–230.

[12] F. Sato, M. Jojo, H. Matsuki, T. Sato, M. Sendoh, K. Ishiyama and K.I. Arai, The operation of a magnetic micromachine for hyperthermia and its exothermic characteristic, 2002 International Magnetics Conference (Intermag, 2002), 28 April–02 May 2002, pp. 3362–3364.
[13] M. Sendoh, K. Ishiyama and K.I. Arai, Direction and individual control of magnetic micromachine, 2002 International Magnetics Conference (Intermag, 2002), 28 April–02 May 2002, pp. 3356–3358.
[14] M. Sendoh, K. Ishiyama, K.I. Arai, M. Jojo, F. Sato and H. Matsuki, Fabrication of magnetic micro-machine for local hyperthermia, 2002 IEEE International Magnetics Conference (Intermag, 2002), 28 April–02 May 2002, FU11.
[15] P.H.T. Uhlherr and R.P. Chhabra, Wall effect for the fall of spheres in cylindrical tubes at high Reynolds number, *Canadian Journal of Chemical Engineering* **73**(6) (1995), 918–923.
[16] F.M. White, *Fluid Mechanics*, 4 edn, McGraw and Hill, 1999.